Identification of Successional Stages and Cover Changes of Tropical Forest Based on Digital Surface Model Analysis

Adilson Berveglieri, Antonio Maria Garcia Tommaselli, Nilton Nobuhiro Imai, Eduardo Augusto Werneck Ribeiro, Raul Borges Guimarães, and Eija Honkavaara

***Abstract*—Forests are in a permanent state of change due to natural and anthropogenic processes. Long-term time series analysis makes it possible to reconstruct the forest history and perform a multitemporal analysis on the cause and effect of changes. This paper describes an approach for successional stage classification in a tropical forest based on vertical structure variations. Stereophotogrammetry and novel image matching methods are used to produce dense digital surface models (DSMs) from optical images (historical and contemporary). An approach was developed to classify the successional stages of trees using local height variations provided by a DSM and image intensity values. Experiments were performed in a semi-deciduous tropical forest fragment located in the West of São Paulo State, Brazil. Six test sample plots and a line transect were established and field surveys were conducted to collect forest variables. These variables were used to characterize and validate five successional classes based on secondary tree species that stratify the forest canopy. The current status of the entire forest fragment was characterized using recent photogrammetric imagery, and a map of historical successional stages was established by analyzing the historical photogrammetric imagery. The investigation demonstrated that the proposed technique can be used to reconstruct the geometric structure of a forest canopy from aerial images. The successional stages can be identified and compared over time using multitemporal photogrammetric imagery and DSMs, which enables an analysis of forest cover changes. The results indicated that the successional stage has changed dramatically during the 50 years period of time.**

***Index Terms*—Forestry, image texture analysis, photography, remote sensing, vegetation mapping.**

Manuscript received February 29, 2016; revised July 1, 2016; accepted August 30, 2016. Date of publication September 19, 2016; date of current version November 30, 2016. The work was supported by the São Paulo Research Foundation (FAPESP) under Grant 2012/23259-9, Grant 2013/50426-4, and Grant 2014/05033-7. *(Corresponding author: Adilson Berveglieri.)*

A. Berveglieri is with the Graduation Program in Cartographic Sciences, Department of Cartography, Universidade Estadual Paulista Julio de Mesquita Filho, Presidente Prudente 19060-900, Brazil (e-mail: adilsonberveg@gmail.com).

A. M. G. Tommaseli and N. N. Imai are with the Department of Cartography, Universidade Estadual Paulista Julio de Mesquita Filho, Presidente Prudente 19060-900, Brazil (e-mail: tomaseli@fct.unesp.br; nnimai@fct.unesp.br).

E. A. W. Ribeiro is with Catarinense Federal Institute, São Francisco do Sul 89240-000, Brazil (e-mail: eduwerneck@gmail.com).

R. B. Guimarães is with the Department of Geography, Universidade Estadual Paulista Julio de Mesquita Filho, Presidente Prudente 19060-900, Brazil (e-mail: raul@fct.unesp.br).

E. Honkaavara is with Finnish Geospatial Research Institute FGI, FI-00521 Helsinki, Finland (e-mail: eija.honkavaara@nls.fi).

Color versions of one or more of the figures in this paper are available online at http://ieeexplore.ieee.org.

Digital Object Identifier 10.1109/JSTARS.2016.2606320

I. Introduction

A MAJOR challenge for biodiversity conservation is understanding the spatiotemporal dynamics in an ecological community. Prado Júnior *et al.* [1] comment that most of the studies have been conducted on the basis of ecological variables, including quantitative and qualitative variables. Relevant studies can be highlighted dealing with the relative density and importance value [2], the quadrat method [3], relative dominance and other variables [4], frequency [5] and the diversity index [6], [7].

When considering remnants of semideciduous tropical forests, challenges are also found because the structure of these are characterized by the number of individuals belonging to different families or species, age and diameter classes, which is well-known as the diameter at breast height (DBH). This diameter is essential to identify successional stages of natural vegetation [8]. Tropical forests may have simple canopies or more complex canopies at different heights in the same area [9]. Vertical structure of canopies is as important as that related to forest horizontal structure (e.g., abundance, dominance, frequency). The occupation of niches at different elevations is one of the crucial factors explaining the high diversity in tropical forests [10].

Groups of regeneration, of dispersion stages and of maturation periods (based on individual heights) can indicate changes in the composition of plants along the forest succession process [11]. Several studies have recognized the high correlation between the variations of vertical structure with the forest successional stage [12]–[15]. According to Trichon [16], an alteration in the composition of plants at each stage is reflected both in the height variation and in the number of canopy levels in more advanced ecological stages, and a spatiotemporal assessment of forests can also show the processes of canopy changes. However, the vertical structure is less frequently investigated because of difficulties in accurately collecting information in the field. Thus, an alternative would be to use aerial images acquired from different epochs to extract information on the vertical structures.

Aerial images are a valuable source of information that can be useful for analyzing the succession of natural vegetation and they can be combined with field survey data [12]. Variations in vertical structure cause shadows that are recorded in panchromatic images, as well as in color and multispectral images. Thus, one of the attributes that can be analyzed is the image texture because shadows represent spatial variations due to canopy

height variations. This indirect measure provided by texture may be advantageously replaced by variations in canopy height in the object space (3-D model), which are directly related to the degree of complexity of the forest structure.

Significant improvements are taking place in the environmental remote sensing due to the advancement of technologies for capturing geometric and spectral information of forest canopies, e.g., photogrammetric sensors with high-resolution multispectral images, hyperspectral sensors, synthetic aperture radar (SAR) and light detection and ranging (lidar) [17].

Digital photogrammetry and lidar are also efficient techniques for detailed 3-D forest canopy mapping. Lidar is considered the most accurate approach for the measurement of the forest height and related characteristics, because it directly acquires vegetation height and structure, and ground elevation with high accuracy and density [17], [18]–[22]. Technological advances achieved in photogrammetric processing, especially dense image matching, have enabled the generation of dense point clouds comparable to lidar [23], [24]. Multi temporal acquisitions using these technologies enable the estimation of the spatiotemporal growth and changes of forests.

Important advances in analysis of forest vertical structure have been achieved with the combination of polarimetry with interferometry (Pol-InSAR) and also with SAR Tomography (TomoSAR), in which tomographic images of forest canopy can be extracted, e.g., to estimate biomass. In general, SAR technology can provide information on forest vertical structure by estimating parameters like forest height, understory topography, and ground elevation [25]–[28]. Yu *et al*. [29] performed a comparison of different data sources (lidar, airborne stereo images, satellite stereo images, radar) for forest application. All sources demonstrated good potential for forest inventory; the SAR-based methods were the least accurate and the lidar was the most accurate.

For retrospective studies using long-term time series, only optical images are available, which were captured on film with aerial surveying. These aerial images have been used since the early years of the 20th century as the primary source for mapping [30]. Nowadays, archives of film-based images are available in most countries and are essential for time-series studies, providing an important source of data for long-term, high-resolution, multitemporal environmental remote sensing analyzes. Furthermore, aerial stereoscopic imagery enables 3-D measurements to estimate tree canopy structure [24], [31]. Such film images can be scanned and converted into digital images. With a pixel size of 20 μm, images in scales of 1:25 000 will have a ground sample distance (GSD) of 50 cm and those in 1:60 000 will achieve a GSD of 1.2 m. These scales were quite common for medium scale mapping in many countries. The availability of digital stereoscopic images with suitable spatial resolution, obtained after scanning, enables the generation of a dense forest cover DSM. Using novel dense stereo matching techniques, for instance semiglobal matching [32], dense DSMs can be produced with grid spacing around 1 GSD.

The potential of historical images for retrospective studies has been shown in different contexts, such as vegetation change [23], land cover changes [33], archeology [34] and climatic studies [35]. Véga and St-Onge [36] and Nurminen *et al.* [37], for example, conducted studies with approaches integrating lidar and historical images for DSM generation. However, these approaches were dependent both on a reference digital terrain model (DTM) of the study area and accurate georeferencing data to integrate the datasets.

Unfortunately, for large areas in tropical forests, DTMs are not available due to cost and area size. This lack of information makes unfeasible the use of absolute height-based algorithms calculated by subtracting a DTM from a DSM to produce a canopy height model (CHM). Moreover, as lidar is not a long-time technology, it is not a solution for long-term retrospective time series. Even orbital digital images (for instance, Landsat) are not suitable because they are limited to four decades ago, making them unfeasible for long period studies. In addition, their spatial resolution is low (approximately 80 m of GSD – in 1970s) and the orbital imagery does not provide 3-D information due to absence of stereoscopy [38]. SAR-based remote sensing datasets are also limited to a few decades.

Several techniques and algorithms can be applied to classify trees in images using data acquired with recent technologies, such as hyperspectral data [39]. However, when using historical images, acquired by film cameras with later scanning, few possibilities are available to analyze forest changes. If a classification is based on texture and spectral response, the angle of solar illumination and shadows can influence the outcome. Historical panchromatic images, mostly using grayscale, also complicate the classification due to the limited dynamic range and spectral information. Thus, a classification using data from the object space (relative heights extracted from a DSM), along with image information (intensity), is more efficient. This combination should allow the identification of structural variations in vegetation environments, which can complement classic biogeographic measurements. The core concept of the approach introduced in the paper is that local relative height variations of the forest canopy are related to the forest structure and this information can be suitable for forest monitoring. Local analysis of the height variation should be sufficient to evaluate the tropical forest structure, since it is characterized by tree species and ages, which are related to height and diameter of trees.

Objectives of this investigation were to develop an approach to classify and identify changes in successional stages in tropical forest remnants based on the vertical structure variations of the vegetation canopy, which are extracted from multitemporal aerial images, and to assess the methodology using field data. Our hypotheses were that the changes resulting from the natural dynamics can be observed by photogrammetry and remote sensing techniques using optical images (panchromatic spectral range), and a few indicators (presented in Section IV) can be related to the vegetation structure and thus can be used to classify successional stages. The technique could be applied to forest cover reconstruction and classification using historical aerial images, which enables an analysis of changes. This was verified in this study, and the developed techniques will be presented in the following sections.

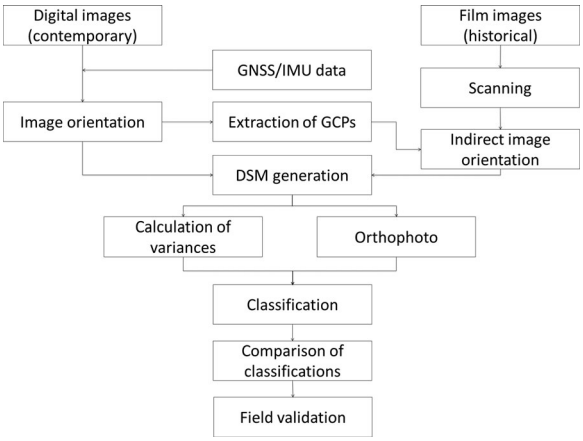

Fig. 1. Photogrammetric workflow for DSM generation, forest cover classification, and analysis of cover changes.

II. Methodology

The aim of the proposed technique is to extract data from optical images, generate a forest canopy DSM and classify successional stages. Using the resulting classification, an analysis of the forest cover can be performed to assess changes.

The data are provided by stereoscopic optical images, which after orientation processing allow DSM generation and calculation of variances to obtain relative canopy heterogeneity information. The photogrammetric techniques enable the reconstruction of the forest height variations using dense image matching.

Fig. 1 presents a flowchart that describes the procedures used to generate 3-D coordinates from optical images and to calculate local height variances. A photogrammetric workflow is shown for two image sets in Fig. 1. The first set refers to contemporary digital images, and the second one refers to historical images based on film (or analog images), depending on the technology used by aerial surveys in past decades.

Digital images are more recent technologies and can be acquired with direct georeferencing. When using historical images, however, a major problem exists related to image orientation. The calibration information and the exterior orientation parameters are often missing.

Korpela [40] demonstrated procedures to orient an image time series using as ground control visually selected immobile points, such as rocks, stones, and roofs of buildings. Additionally, the author commented on the difficulty of identifying multitime real points in forest environments. Véga and St-Onge [36] used a series of 58 years of aerial imaging to reconstruct the forest height growth. The authors verified that the CHMs derived from historical aerial imaging presented a quality sufficient for forest dynamics studies.

Historical images are typically available on film and can be scanned to generate digital images. When the camera calibration certificate is available, the interior orientation step, which is implemented in most commercial photogrammetric software, is enough to correct the existing systematic errors and to correctly reconstruct the incident bundle of rays. However, when the calibration certificate is missing, the systematic errors (film shrinkage, lens distortion) will not be corrected but their effects are usually below 1 pixel.

Another requirement for 3-D retrospective photogrammetric measurements is the determination of the exterior orientation parameters. The photogrammetric method known as bundle block adjustment (BBA) indirectly computes the exterior orientation parameters (coordinates of the camera perspective center and orientation angles). Commonly, BBA uses ground control points (GCPs) that tie image data to the desired cartographic coordinate system (or object coordinate system) and tie points that connect images to each other. The block adjustment is a highly automated process applying automatic image matching methods. Georeferencing is an important phase of this process. Today, global navigation satellite system/inertial measurement unit (GNSS/IMU) systems are used to provide good quality exterior orientation parameters in mainstream photogrammetric production lines. Furthermore, a set of GCPs can be marked on the ground and targeted so that they can be accurately identified and measured in images. In historical images, neither the GNSS/IMU orientation information nor targeted GCPs are available. Because of this lack of information, unchanged distinguishable points must be determined using the photogrammetric point determination technique from a recent, georeferenced image block. A minimum of three GCPs are needed in the area of the image block, but preferably more points are used to improve accuracy and reliability.

With this information, a dense DSM can be generated using image matching algorithms, which use image similarity measures to create 3-D points from two or more overlapping images [32]. Local errors caused by mismatches are checked and excluded with outlier filtering. Remondino *et al.* [41] presented a critical review on recent innovations about dense image-matching methods used for 3-D modeling and mapping. Four photogrammetric packages were assessed that demonstrated considerable potential. After the generation of the DSM, an orthophoto mosaic is calculated using the airborne images, orientation information and the DSM. An orthophoto is a georeferenced product in which all points have the same scale. Thus, two orthophotos of the same area produced from aerial photos taken at different times should match.

The next phase in the process is the classification of the forest successional stage using the DSM and pixel intensity values. A sliding window is applied over the DSM and the height variances are calculated for each window. The digital numbers (DN) [42, p. 54] (the pixel intensity in discrete numbers) are extracted from the orthophoto. The combination of variance ranges and DN intensity levels enables the definition of classes which represent groups with similar characteristics, which are visible in the photogrammetric data. This classification aims at correlating the vertical geometric features, identified in the DSM and DN intensity, with the forest successional stages, which form and change the canopy over time. In addition, the classification from each epoch can be compared to assess the forest cover changes. Finally, a field survey is performed to validate the results.

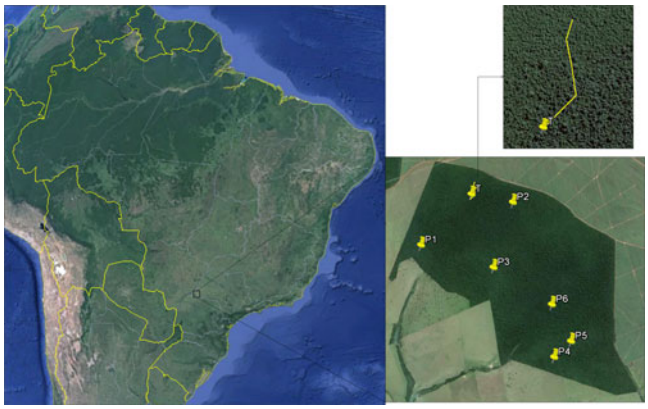

Fig. 2. Location of the Ponte Branca fragment in Brazil and the distribution of plots and line transects used for sampling. Source: Google Earth.

III. Materials and Experiments

The proposed procedures were applied to contemporary images and historical images. The study area was composed of remaining forest with well-preserved regions and areas where the vegetation had been removed.

A. Study Area

Ponte Branca is a remaining fragment of a semideciduous forest located in the West of São Paulo State, Brazil (22°24′51″S and 52°30′50″W) (shown in Fig. 2).

The forest structure contains multiple canopies that support a rich vegetation diversity, which can be characterized as alluvial (riparian forest) or submontane, depending on the altitude, which ranges from 350 to 450 m. The dominant vegetation is composed of species like *Dilodendon bipinnatum*, *Eugenia piriformis* and *Termimalia triflora* in the lower canopy layer and species *Apuleia leiocarpa*, *Copaifera langsdorffii* and *Hymenaea L.* in the higher canopy layer. The surrounding vegetation is composed of pasture (south and west) and sugarcane plantation (north and east). This study area was selected for experimentation due to its diversity of species, different successional stages, and regeneration areas. The fragment is a dense tropical forest composed of native trees with an area of approximately 13 km^2. It is part of a federal protected reserve named *Estação Ecológica Mico-Leão-Preto* and is protected by environmental laws.

B. Imagery

Two image blocks, which are detailed in Table I, were used in the experiments. The first block is composed of four digital aerial images (in RGB) of the study area collected by the Topocart Company in 2010. The calibrated interior orientation parameters were provided, as well as the exterior orientation parameters collected with direct georeferencing and refined with BBA with GCPs. The specifications of the cameras used are presented in Table II.

The historical image block (see Tables I and II) is composed of six panchromatic images that were collected by the Prospec Company in 1962 using a Zeiss film-based camera. Interior orientation parameters and exterior orientation parameters were not available. Only the focal length of 152.98 mm was known. The negatives (provided by the Base Company) were digitized with a photogrammetric scanner (UltraScan 5000 – Vexcel Imaging GmbH, Graz, Austria) with a pixel size of 21 μm, which resulted in an average GSD of 55 cm. Due to the lack of the camera calibration certificate, only a rigid body transformation to the fiducial center was conducted. The principal point displacement related to the fiducial center, the lens distortion, and the film shrinkage were not corrected due to the lack of the calibration data, but the effect of these corrections is usually less than 21 μm, which is the pixel size.

TABLE I
Details of the Image Blocks Used in the Experiments

Camera model	Flying height (km)	Image scale	Image forward overlap	Number of images	GSD (m)	Year
Digital UltraCam - Vexcel	7.5	1:75 K	60%	4	0.45	2010
Zeiss film-based camera	3.7	1:25 K	63%	6	0.55	1962

TABLE II
Camera Information

Camera model	Focal length (mm)	Image format	Number of fiducial marks	Type of sensor
Digital UltraCam Xp – Vexcel	100.50	17 310 × 11 310 pixels	-	Digital with pixel size of 6 μm
Zeiss film-based camera	152.98	23 × 23 cm	4	Film – Kodak Super XX

C. Field Data

Field surveys were conducted to collect data in seven sample areas in the Ponte Branca fragment. The field data enabled the characterization of the successional stages of each sample relating them to the vertical variation classes presented in Section IV. The sample areas were also used to validate the classes. The field survey data show the forest status in 2015, and it is assumed to be valid also for the images acquired in 2010. For the classification in 1962, an inference to describe the historical status can be made using the similarities among classes determined between epochs in Section IV-A.

Fig. 2 shows the plot locations used for sampling, and Fig. 3(a)–(c) are examples of vegetation cover collected from different views in the study area.

The plot size and shape were defined following methodologies applied to Brazilian tropical forests, as discussed by Durigan [43]. This author also comments that a square shape enables a better sampling of the spatial distribution of species. For field surveys, the plots 1-6 were square patches with dimensions of 40 m × 40 m at distances from the border of 230, 560, 530, 210, 680, and 1200 m, respectively. Plot 7 was surveyed

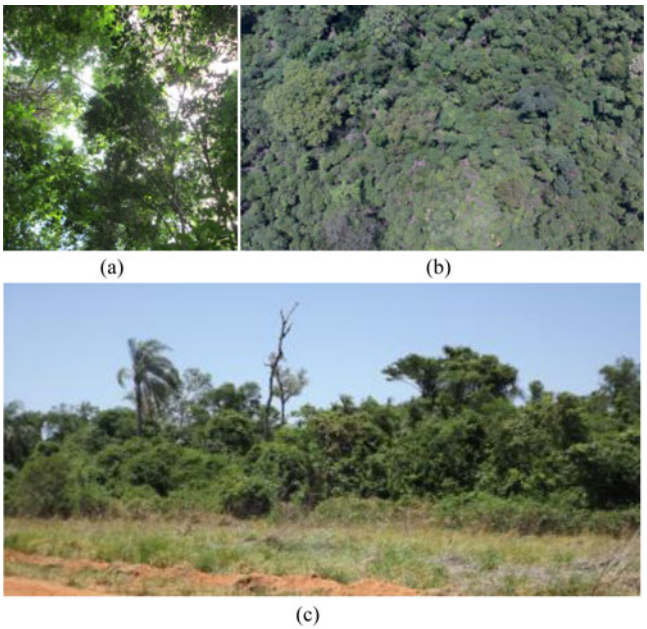

Fig. 3. Examples of forest cover: (a) internal view, (b) aerial view, and (c) external view.

TABLE III
FOREST DATA COLLECTED BY FIELD SURVEYS

	Plot 1	Plot 2	Plot 3	Plot 4	Plot 5	Plot 6	Line transect
Number of trees	411	277	418	490	352	167	1089
Number of tree species	14	22	23	24	14	20	27
Average altitude (m)	357	409	407	385	398	386	412

with a line transect of approximately 450 m $\times$ 10 m, approximately 280 m from the border. The transect length was defined to include a sufficient number of different cover classes, and this area was defined based on the classification analysis (Section IV). This field survey was conducted with transect shapes to better assess the transitions between classes, given a continuous corridor with cover variations.

Based on the vegetation characteristics inside the plots, the minimum DBH value $>$3.8 cm (or circumference $\geq$12 cm) was defined as the threshold to select significant trees for sampling. Ground elevations were also measured by GPS receiver within the plots and transect to obtain a local altitude reference. The species, spatial position, and DBH were also recorded. Species identification was aided by a forester who was a local inhabitant; the species were later verified and specified by their scientific names.

Table III shows the number of individual trees and species and the average local altitude collected in the field surveys. A total of 3204 trees were surveyed, and a range of 14-27 species were identified in the samples.

D. Successional Stages

Key aspects for identifying the successional stages of sampling areas are the relative number of shade intolerant species and DBH. The analysis of field data, considering the relative proportion of some species together with their average DBH, was the main parameter used to identify the successional stage of each plot. Thus, the successional stages were related to the species, which determine the forest vertical structure, and were characterized as pioneer, early secondary, late secondary, and climax stages. The characterization of each stage was adapted from current Brazilian laws. The criteria that were used are described as follows:

1) Primary regeneration stage (pioneer): the physiognomy initially has a predominance of herbaceous strata and can present shrub strata that occur with a predominance of one over the other. The shrub strata can be open or closed and are prone to present a uniform height in individuals of dominant species, generally up to 2 m. The shrubs have a DBH of approximately 3 cm and do not generate a woody product. Biological diversity is low, with few dominant species.
2) Initial regeneration stage (early secondary): woody plants have DBH up to 10 cm. Saplings of tree species of mature stages may appear in the understory. The biological diversity is low, consisting of approximately ten dominant tree or shrub species.
3) Medium regeneration stage (late secondary): forest physiognomy with several tree sizes and the presence of different height layers. Each layer has a cover varying from open to close. The surface of the upper layer can be uniform, and trees tolerant to the absence of light can appear. The average DBH of tree species in their mature stages can reach a value of 20 cm. Biological diversity is significant. In some cases, the dominance of a few species can occur, generally those with rapid growth. In addition, palm trees may be growing.
4) Advanced regeneration stage (climax): there are large numbers of strata with trees, shrubs, terrestrial herbs, vines, etc., in which the abundance and number of species vary depending on the climate and location. The upper canopies are generally extensive. The average DBH is always greater than 20 cm. The diametric distribution has a great range, providing a significant amount of woody product. The biological diversity is high due to the structural complexity and the number of species.

The pioneer and early secondary (primary succession) stages produce the lowest structures of the forest, forming the understory. The late secondary and climax are responsible for stratifying the forest in different layers over time, producing variations of canopy heights. Thus, the basis for validation and specification of successional stages is explained by the species that modify the forest vertical structure – secondary succession. A study performed by Vieira *et al.* [44] verified the covariance of height and DBH of trees with successional stages for different groups using tree age in a forest of eastern Amazônia. The technique was based on Landsat spectral properties and ecological variables. The authors concluded that such variables can stratify the forest with spectral properties. Thus, this statement was adopted in this approach to correlate forest data collected in field to data extracted from aerial images.

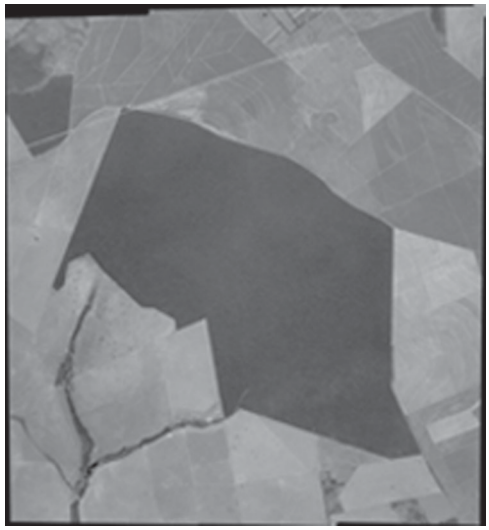

Fig. 4. Orthomosaic generated with the contemporary image block (in 2010).

E. Photogrammetric Images and Processing

Photogrammetric processing was performed using ERDAS Imagine-LPS software Version 2015 (Hexagon Geospatial, Norcross, GA, USA), which is a professional photogrammetric software allowing accurate self-calibrating BBA and automatic DSM and orthomosaic generation.

The RGB images of the photogrammetric block (2010) were converted to the IHS system, and only the I band (intensity) was used in the experiments. This conversion was effective for comparison with panchromatic historical images.

The exterior orientation parameters of the RGB image block were supplied by the Topocart Company, along with the image and the corresponding data. The exterior orientations were calculated by the Topocart Company using direct georeferencing refined by BBA with INPHO software. These exterior orientation parameters were imported into LPS software. Subsequently, tie points were generated, and the ground coordinates of these tie points were computed by BBA. From this set of data, a dense DSM was produced, and then an orthomosaic of the study area was generated. In addition, the 3-D coordinates of six conjugate points (estimated as tie points in the BBA of the contemporary images) in the historical block were also determined. Fig. 4 shows an orthomosaic produced with the images of the I band.

The historical images [see Fig. 5(a)] were indirectly oriented with the following settings: the fixed interior orientation parameters, the initial exterior orientation parameters based on approximate camera positions, and the GCPs in the object space, with a standard deviation of 0.5 m and point coordinates in the image space with a standard deviation of 0.5 pixels. Three points were used as full GCPs, and three others, as altimetry control; their coordinates were determined using the RGB block captured in 2010. The tie points were automatically generated using 25 points per model. In each model, distinguishable points were detected based on the analysis of local bidirectional grey level gradients and transferred to the overlapping images by correlation with refinement by least squares algorithm.

The BBA, with ERDAS-LPS software, was used to determine the image orientations. The root mean square errors (RMSEs)

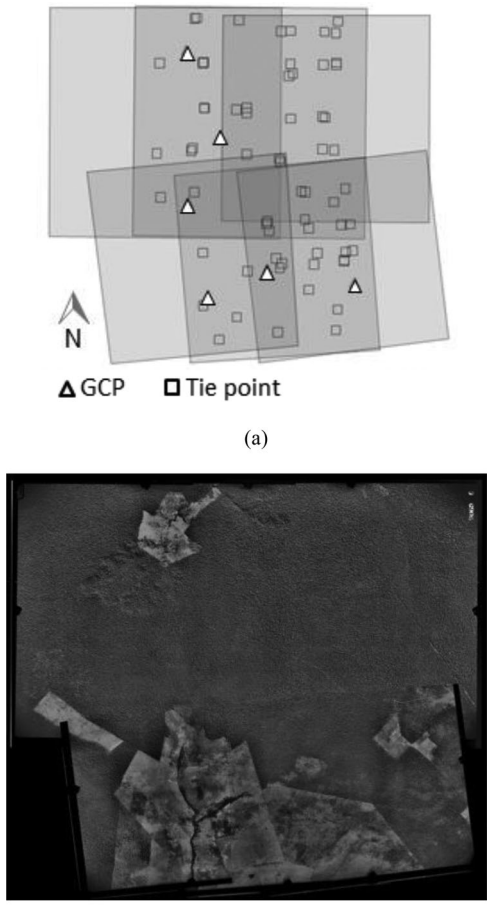

Fig. 5. Historical image block (in 1962) composed of (a) six GCPs and several automatic tie points. (b) Orthomosaic.

of the GCPs were 0.56 cm in X, 1.51 cm in Y, and 15.6 cm in Z. In the image space, the RMSEs in xy were approximately 0.7 pixels. These results were acceptable for further use in this investigation. Fig. 5(b) displays the historical orthomosaic of the study area.

In the next step, dense DSMs were produced for both image blocks using the automatic terrain extraction technique of the LPS software using existing matching strategy for forest areas. This strategy used a search window size of 17×3 to differentiate and correlate similar features. A grid spacing of 1 GSD was used in both blocks, providing a grid DSM with spacing of 55 and 45 cm for the 1962 and 2010 data, respectively.

Fig. 6(a), (b) present both DSMs for the study area. Two profile lines were extracted from each DSM in similar positions to show the characteristics in 1962 [see Fig. 6(c)] and 2010 [see Fig. 6(d)] from which forest cover changes can be observed over time. Although the GSDs are not the same, the small difference between them ensures an approximate scale to perform a comparison of the results. In this technique, only variations of local heights within the same block are used. It is not necessary to register time series grids.

Orthomosaics were produced for the two blocks for the study area with the same DSM dimensions for both images. For the 2010 imagery, histogram matching was used; for the 1962 data,

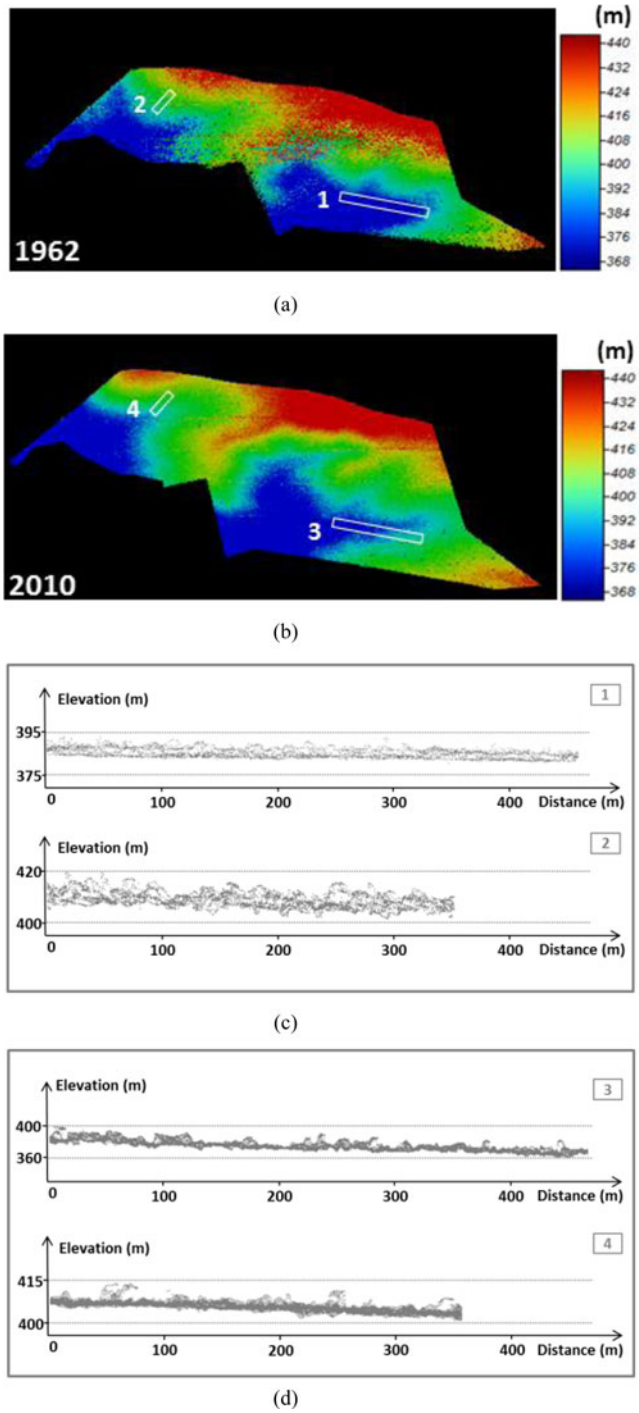

Fig. 6. DSMs produced with the (a) historical image block and (b) RGB image block. Four profiles (numbered 1 to 4) ranging 350–500 m in length were extracted. They are presented in (c) for 1962 and in (d) for 2010.

a vignetting correction was performed to reduce the variations in image brightness. Vignetting effect makes areas in the image center brighter and edges darker due to a combined effect of lens falloff and light travel distance [42, p.25].

The purpose was to use the DN intensity as additional information for the classification considering the forest brightness response.

TABLE IV
RANGES OF VALUES COMBINING HEIGHT VARIANCE AND DN INTENSITY FOR CLASS GENERATION

Class	Combination	Height variance (m^2)	DN intensity [0–255]
I	High variance	>30	0–255
II	Medium variance and high DN intensity	7–30	95–255
III	Medium variance and medium DN intensity	7–30	80–94
IV	Medium variance and low DN intensity	7–30	0–79
V	Low variance	<7	0–255

F. Classification

The forest cover classification was performed using in-house developed software (implemented in C/C++ language). In the algorithm, a convolution window was used to compute the local height variance from the DSM using a pre-defined size based on the sample size surveyed in the field. The window size was set to one quarter (approximately 20 m $\times$ 20 m) of the sample plot. This guaranteed several subsamples within the plots for assessment of outputs. A median filter was also applied to smooth the results.

Due to the heterogeneity of the Ponte Branca fragment, the classes were defined empirically. First, a multilevel histogram thresholding [45] based on an adapted Otsu's method was applied to the height variance values to identify a number of distinguishable classes. Then, the class ranges were fine-tuned based on the resulting spatial distribution (class homogeneity). To improve the class distinctness, the DN intensity extracted from the orthomosaic was adopted as complementary Boolean information for decision making in intermediate classes. Both the height variance and the DN intensity were used with clustering-based image thresholding (segmentation of the classes) using in-house developed software.

Five classes were defined by combining high, medium, and low variance with high, medium, and low DN intensity. These combinations resulted in the following most significant numerical classes for a description of the forest cover, as shown in Table IV.

IV. RESULTS AND DISCUSSION

A. Results of the Forest Classification

The classification technique was applied to both the historical and RGB blocks, and the results are presented in Fig. 7(a), (b). It was not feasible to define the same five classes for both epochs. Only two classes presented the same features (Classes I and III corresponding to HistClass I and II), which was expected due to changes that occurred in the forest over time, mainly from human interference. The ranges of variances between both DSMs were proportionally defined among the classes from 2010 in relation to 1962. Otsu's method for thresholding was also applied to the historical images, which determined the ranges of DN intensity. In addition to the two similar classes between both epochs, two others were identified in 1962, which were a border

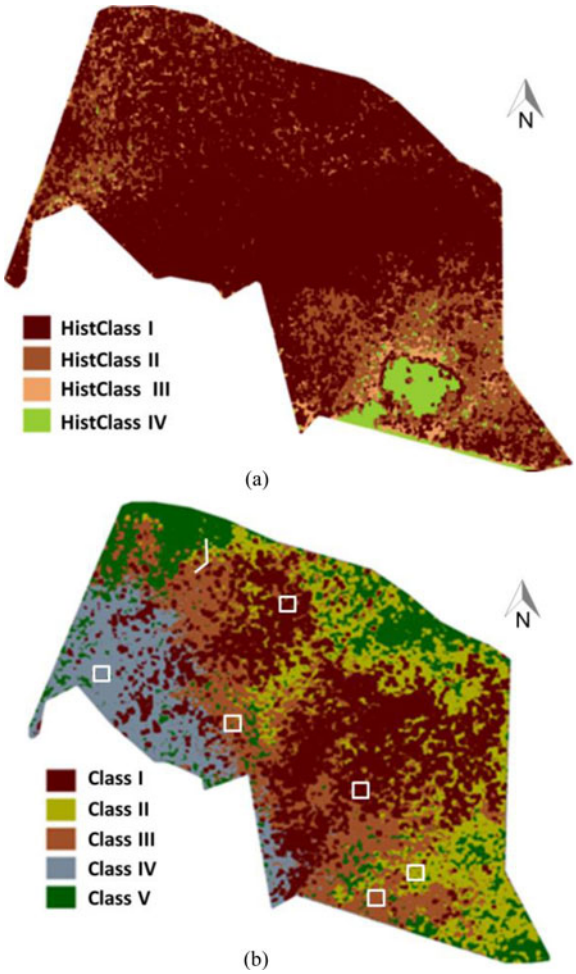

Fig. 7. Forest cover classification in (a) 1962 and (b) 2010, this last indicating sample plots (square) and transect (line) locations.

effect in the historical class (HistClass III) and a deforestation area (HistClass IV) as a low variance class.

Thus, the classification was made for the Ponte Branca fragment with the images acquired in 1962, being the historical classes (HistClass) related to the forest cover are as follows HistClass I to IV. For the classification of the Ponte Branca fragment in 2010, the contemporary classes were labeled as follows Class I to V. These classes will be described and discussed in Section IV-B after validation with field data.

Some factors can be identified as probable causes of changes which help interpret forest cover changes. It is important to highlight that the evaluation of the causes of those changes is beyond the scope of this paper. The main aim is to introduce and assess an approach to classify successional stages in tropical forests using historical images, which enables the identification of cover changes.

As presented in Fig. 8(a), in 1962, most of the area surrounding the fragment was formed by native forest, with a pasture presenting only in the southern part. A few areas also showed cutting patterns, which indicated a deforestation process. Over five decades, almost the entire area, which had been occupied by forest, was replaced by agriculture (sugarcane, in 2010), as shown in Fig. 8(b).

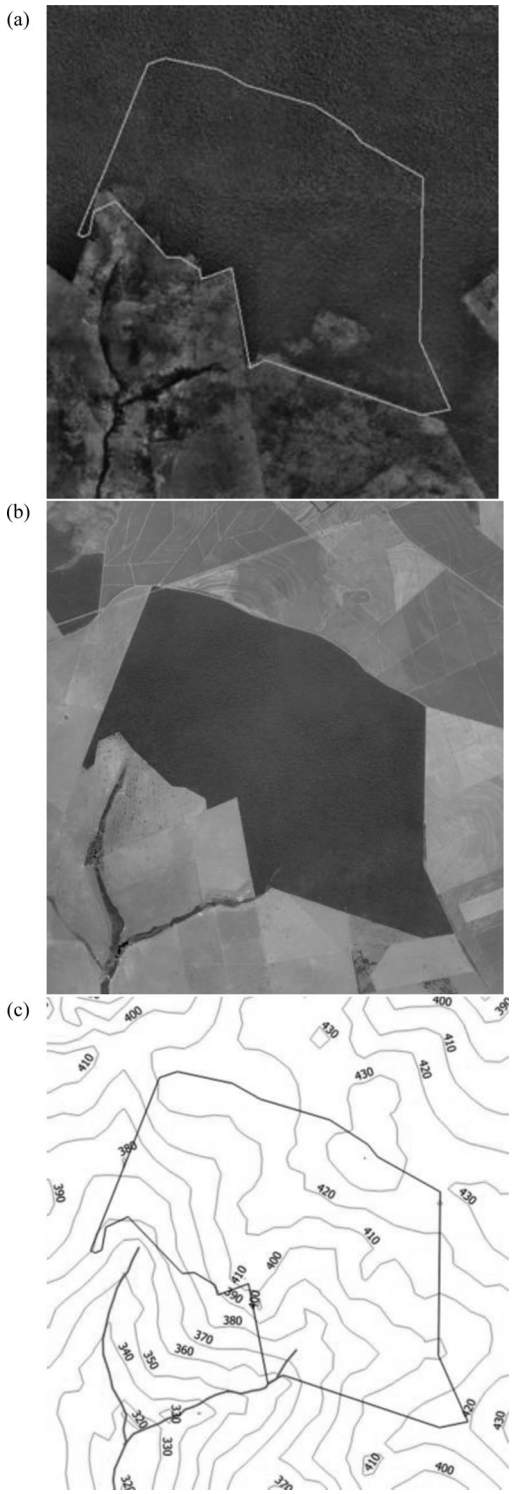

Fig. 8. Ponte Branca fragment with its surroundings in (a) 1962 and (b) 2010. (c) Elevation contours of the study area with two water springs in the southern part.

In addition to the occurrence of deforestation (including the clear cutting inside of the fragment), border effects resulting from fires and the application of agricultural chemicals on the farmed area also caused changes to the forest cover. Furthermore, the Ponte Branca fragment is located near (approxi-

mately 20 km) a hydropower reservoir, where studies performed by Albuquerque Filho and Leite [46] also indicated a rising groundwater level. Chang [47] noted that deforestation can alter the groundwater level, raising it in relation to the surface. These factors can cause changes in forests due to an increase in the humidity of the soil. The comparison between the images in Fig. 8(a), (b) is evidence of the displacement of two water springs in the fragment 8(c), which indicates a possible higher groundwater level.

B. Analysis of Field Data

The plots were determined following the classification produced in Section IV-A (Classes I-V) and the collected field data were used to describe each class in relation to the successional stages based on secondary tree species and DBH.

First, the heterogeneity of the classes was measured by the Shannon-Wiener diversity index (*H*) of the observed trees based on the proportional abundances of species as proposed by Turner [48] using (1):

$$H = -\sum_{i=1}^{s} p_i \ln p_i \tag{1}$$

where *i* is a tree species; *s* is the number of tree species sampled; nd $p_i = n_i/N$ is the proportion of each species (n_i) in relation to the total number of trees (*N*). The resulting indices were, respectively, $H =$ 1.7; 1.8; 1.5; 1.6, and 1.7 for Classes I to V, indicating that all plots are heterogeneous with index $\geq$ 1.5, since several species were identified, as presented in Table III.

In the field surveys, all trees above the established threshold were identified and measured to obtain the DBH. This DBH was essential for distinguishing the vertical growth ranges of the trees tolerant to the absence of light without requiring the tree height, since the DBH increase is related to the vertical growth of secondary species. An average DBH was calculated using all sampled trees, resulting in a DBH = 11 cm, which was used as a threshold for counting the number of secondary trees with the DBH >11 cm. The purpose was to extract the taller trees of secondary species to separate the higher canopy.

The analysis on the secondary tree species is important because such species alter the forest vertical structure. The tree species with DBH < 11 cm in this study form the lower forest canopy (or understory), where all tree species are mixed. Over time secondary species grow forming the highest levels of forest elevation and stand out in relation to the pioneer and early secondary species. Fig. 9 shows the average DBH in the five classes considering all tree species (of all successional stages) with a DBH >11 cm.

Classes IV and V indicated larger values because they are, for the most part, composed of primary succession trees, which is reflected in the average calculation. Class I also showed the largest standard deviation, which represents the existence of trees in more advanced successional stages.

The graph in Fig. 10 shows the average DBH values of only secondary species with diameters larger than the mean of 11 cm. Class I indicated the largest DBHs (>35 cm) and also a high standard deviation (>20 cm), representing a set of tall secondary

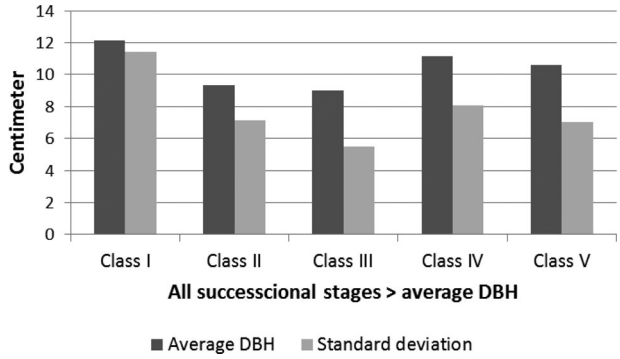

Fig. 9. Average DBH of all species in the five classes.

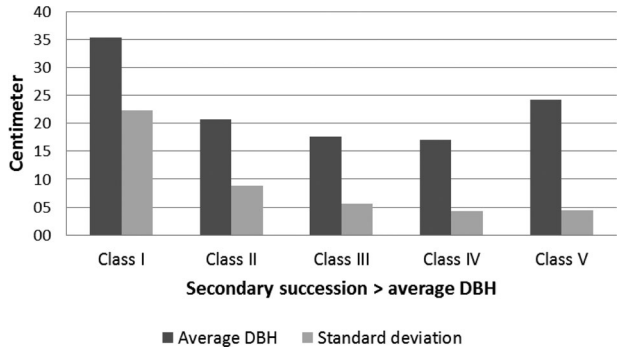

Fig. 10. Average DBH of secondary species with a DBH >11 cm.

trees in the highest canopy level. Class II presented secondary species standing out in relation to the understory due to the standard deviation (>9 cm), but fewer tall trees were found in comparison to Class I. Classes III and IV showed similarity, their values were smaller (<18 cm) than other classes. Class V indicated groups of secondary species with DBH close to 25 cm and with small variation of DBH (standard deviation <5 cm). If both graphs are compared, it can be seen that Classes IV and V are significantly composed of primary species. Classes IV and V in Fig. 9 presented DBHs larger than Classes II and III. The DBHs of these classes in Fig. 10 did not indicate the same graphical behavior, mainly for Class IV that resulted in the smallest value, representing fewer tall secondary trees in comparison to the other classes.

The overall density (primary and secondary species) was calculated for each class. The relation between the number of trees per area unit – hectare (ha) – showed minor differences among the values in Classes II to V (densities 1988; 2392; 2093; and 2200 trees/ha, respectively), except in Class V, where the density was 1288 trees/ha, which is lower due to the predominance of larger trees.

Considering only the secondary tree species >average DBH, the graph in Fig. 11 was generated using three ranges of DBH values to show the density of tall trees. Classes I, II and III presented higher densities (>100 trees/ha) when considering a DBH >11 cm. The highest densities of tall trees with a DBH greater than 22/33 cm were significantly more common in Class I (65 and 44 trees/ha for the DBH 22 and 33 cm, respectively). Classes II and III were characterized by high densities of secondary trees with DBH >11 cm (>150 tree/ha),

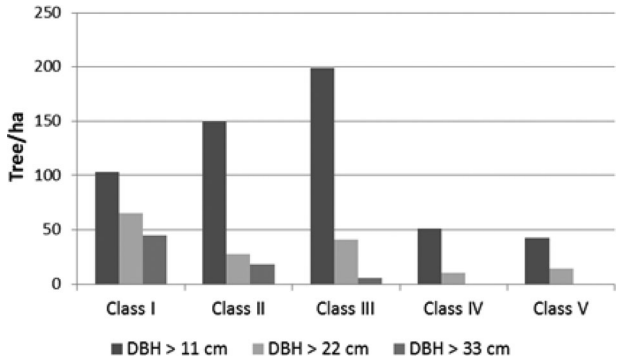

Fig. 11. Density (tree/ha) of secondary species considering three values above the overall DBH.

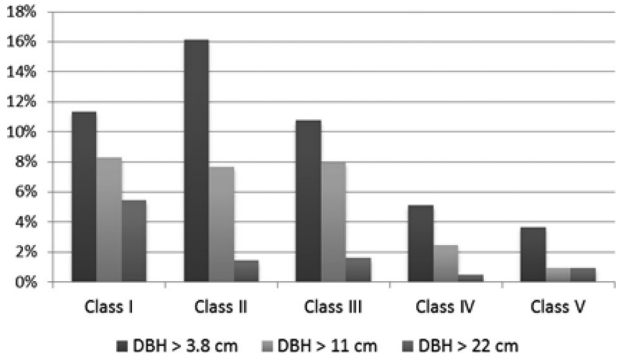

Fig. 12. Percentage of secondary trees in each class considering the three DBH ranges.

mainly Class III that also presented a higher density of trees with DBH >22 cm but less for DBH >33 cm. In Classes IV and V, there were no trees with a DBH >33 cm, the number of trees with a DBH >22 cm was low and with DBH >11 cm was also smaller than the other classes. Therefore, both classes IV and V were composed of smaller secondary trees, resulting in a low density of tall trees. Class I had the highest densities of all three DBH ranges.

Another analysis was made based on the proportion of the number of secondary trees compared with the total number of trees inside the plots. Fig. 12 shows the proportion in percentage of the five classes considering the secondary species at three intervals of DBH: the first (DBH >3.8 cm) refers to the minimum DBH from which the trees were sampled; the second (DBH >11 cm) is the overall diameter calculated from all the trees surveyed in field; the third (DBH >22 cm) is double the overall DBH, which was used to better separate taller trees within each class.

As seen in Fig. 12, Class I had high percentage of secondary species, ranging from short trees (>10%) up to the highest trees (approximately 5%). The proportion of tall trees with DBH >11 cm was approximately 8%. Class II presented the highest proportion with DBH >3.8 cm (16%), indicating the large number of young secondary trees. For a DBH >11 cm, the proportion was approximately 5% and with a DBH >22 cm was smaller than 2%. Class III was an intermediate category of tall trees, which was mainly formed by a proportion of trees with a DBH >11 cm (approximately 8%) but a low number of trees with a DBH >22 cm (< 2%). The smallest proportion of secondary tree species was in Class V (< 4%). Class IV had the second lowest proportion of secondary species (approximately 5%) and had a higher percentage of tall trees with a DBH >11 cm compared with Class V.

In general, Class I was a clustering of taller trees and had the greatest percentage of secondary species, ranging from short trees up to the highest trees. In contrast, Class V presented the smallest number of these species, being that the vertical structure was predominantly determined by short trees. Although the percentages do not seem as expressive, it is important to highlight that secondary tree species occupy significant space inside the forest due to their basal area size. Thus, the number of tall trees is expected to be low. The existence of secondary species in mature stage is also an indicator of the forest conservation status, since a long time and good environmental conditions are required.

C. Analysis of Forest Cover Classification

From the field surveys, the classes obtained with the proposed technique were related to statistical data to characterize each successional stage in the Ponte Branca Fragment. Thus, using the main observed characteristics, the five forest classes previously presented in Section IV-A (epoch 2010) can be explained with respect to the vertical structure, as presented in Table V.

All plots presented heterogeneity index >1.5, but this index itself is not sufficient to differentiate the Classes I to V. It only confirms the tree species diversity in the study area. Thus, the other forest variables including DBH, density, and proportion were used to characterize each class. The existence of bromeliads is taken into consideration in Class IV. These were noticed in the sample area and indicate a humid soil, appearing in the aerial images as a vegetation area with low DN intensity. This shows the need to use the DN intensity as an additional attribute for the forest cover classification.

To establish a relationship with the characterization adapted from Brazilian laws (presented in Section IV-A), Classes I-V can be approximately related as:

1) Class I: has characteristics approaching to a climax stage or advanced regeneration stage;
2) Class II: presents many young trees in a primary regeneration stage;
3) Class III: contains many trees in medium regeneration stage;
4) Class IV: presents trees in initial regeneration stage; and
5) Class V: presents trees in initial regeneration stage.

It is important to note that this relationship is only an approximation, because Brazilian forests constitute heterogeneous environments and rules defined for a type of environment do not apply exactly to another type. The classes in Table V and Fig. 7(b) represent the current successional stage in the Ponte Branca fragment, which is continuously changing due to natural environmental dynamics.

For the classification in 1962, as presented in Section IV-A, two classes (I and III) were similarly obtained between 1962 and

TABLE V
SUMMARY OF THE FOREST COVER CLASSIFICATION (IN 2010) BASED ON THE SECONDARY SPECIES AND THE FIELD SURVEY

	Class I	Class II	Class III	Class IV*	Class V
Diversity	Heterogeneous > 1.5	Heterogeneous > 1.5	Heterogeneous > 1.5	Heterogeneous > 1.5	Heterogeneous > 1.5
DBH	Predominance of secondary species of mature age. This class represents the trees achieving the highest canopy layer.	Predominance of secondary species, which are between young and intermediate age.	The predominance of primary species decreases in relation to the secondary species, which have not yet achieved mature age.	Predominance of primary species containing few mature trees. Secondary species with predominance of young trees.	Predominance of primary species containing some mature trees. Secondary species with predominance of young trees.
Density	High density of tall secondary trees all canopy layers.	High density of tall secondary trees in the lower canopy layer, and low density in the intermediate and highest canopy layers.	High density of secondary species in the lower canopy layer and moderate density in the intermediate canopy layer.	Low density of secondary species in the intermediate canopy layer. There are almost no secondary trees in the highest canopy.	Low density of secondary species in the intermediate canopy layer. There are almost no secondary trees in the highest canopy.
Proportion	High proportion of low, medium and tall trees in all canopy layers.	High proportion of secondary trees in the lower and intermediate canopy layers. Low proportion of tall trees in the highest canopy layer.	High proportion of lower secondary trees. Moderate proportion of medium trees and low proportion of tall trees.	Moderate proportion of secondary trees in the lower canopy. Low proportion of medium trees in the intermediate canopy layer.	Moderate proportion of secondary trees in the lower canopy. Low proportion of medium and tall trees in the intermediate canopy layer.

(*) Existence of bromeliads inside the area, which indicates a humid soil.

2010 [see Fig. 7(a), (b)], determined by the forest cover classification from the DSMs and images. This enables an inference for retrospective classification in 1962 as follows:

1) HistClass I: similar to Class I in 2010. This class represents the greatest part of the forest, indicating homogeneous regions with mature species in 1962. The number of mature trees has dramatically reduced during the period of 50 years;
2) HistClass II: similar to Class III in 2010. This class is formed by trees with medium height variance, which can indicate tree extraction at an early stage. In 2010, this area shows a regeneration stage because of the tree growth;
3) HistClass III: a transition effect can be observed between HistClass I and II;
4) HistClass IV: shrubs can be inferred in this region due to a deforestation caused by human action in 1962. A homogeneous area is shown. In 2010, this area has also presented a regeneration stage.

Thus, the forest cover can be reconstructed historically, and changes can be verified over time. As can be seen in 1962, medium and advanced regeneration stages were predominant, indicating a forest with mature age and homogeneous areas. In addition to the natural dynamics of vegetation, man-made events have produced a drastic change in the canopy structure over five decades. In 2010, the forest conservation status presented a canopy structure stratified in several layers with different regeneration stages. This status showed the Ponte Branca fragment within a forest regeneration cycle, in which many areas are composed of young trees.

V. CONCLUSION

A novel methodology based on dense image matching technologies for forest canopy classification following the successional stage was presented and assessed in this paper. Several techniques were combined to use the local height variance obtained from 3-D models (DSM), which is different of calculating variances from grey level image textures, commonly done by existing software. Due to the difficulties of conducting field surveys to acquire data on forest vertical structure, the study presented a technique requiring only stereoscopic aerial images, including application for retrospective studies to reconstruct forest covers.

The experiments showed a correlation between forest vertical structure (based on DSM) and successional stage, which varies with the composition of vegetation at each stage. Six ground sample plots and one transect were established in a semideciduous forest located in the West of São Paulo State, Brazil. Forest variables (species and DBH) and diversity indices (diversity, relative density and proportion of tall trees) were analyzed in several samples surveyed in the field. The forest characterization based on variables and indices of secondary species allowed a description of the successional stage classes. Such field indicators presented a relationship to the forest vertical structure visible in the aerial images. Thus, the data that relate DN and height variance extracted from images can be correlated with forest variables allowing the definition of the status of a forest successional stage.

The classification performed for two different years (1962 and 2010) enabled an analysis of the forest cover changes (Section IV). In 1962, homogeneous areas with trees in mature age were predominant, but natural and anthropic actions have changed the canopy structure during five decades, causing an environmental degradation. In 2010, five canopy layers were identified to represent the forest status, presenting from primary regeneration stage to advanced regeneration stage. The classification showed the forest in a natural regeneration cycle.

The technique was applied to a study area where the relief presents low variations (range of 70 m in elevation change). For areas with high relief variations, a normalization process to an average elevation should be conducted. In addition, the proposed techniques do not depend on reference DTMs and do not require extensive field surveying inside the forest, which is a laborious and hard task in tropical forests. Another possible application for this technique is to use it as a support for field survey planning, which could be guided by the classification based on remote sensing. Plot locations can be better planned following the previously identified characteristics.

ACKNOWLEDGMENT

The authors are sincerely thankful to the São Paulo Research Foundation – FAPESP for financial support. The authors are also grateful to Base Aerofotogrametria and Topocart Companies for providing aerial images and to Baltazar Casagrande, Gabriela Miyoshi, Mariana Thomaz and Valter Campos for their assistance with the field surveys.

REFERENCES

[1] J. A. Prado Júnior *et al.*, "Fitossociologia, caracterização sucessional e síndromes de dispersão da comunidade arbórea de remanescente urbano de floresta estacional semidecidual em Monte Carmelo, Minas Gerais," *Rodriguésia*, vol. 63, no. 3, pp. 489–499, 2012.

[2] J. T. Curtis and R. P. McIntosh, "The interrelations of certain analytic and synthetic phytosociological characters," *Ecology*, vol. 31, no. 3, pp. 434–455, 1950.

[3] G. Cottan and J. T. Curtis, "The use of distance measures in phytosociological sampling," *Ecology*, vol. 37, no. 3, pp. 451–460, 1956.

[4] D. Mueller-Dombois and H. Ellenberg, *Aims and Methods of Vegetation Ecology*. New York, NY, USA: Wiley, 1974.

[5] S. B. Chapman, *Methods in Plant Ecology*. New York, NY, USA: Wiley, 1976.

[6] A. Krebs, "Levantamento fitossociológico da formação - mata do Morro do Coco," *Iheringia Sér. Botânica*, vol. 23, pp. 65–108, 1978.

[7] P. Greig-Smith, *Quantitative Plant Ecology*, 3rd ed. Oxford, U.K.: Blackwell, 1983.

[8] V. S. Vale *et al.*, "Functional groups in a semideciduous seasonal forest in Southeastern Brazil," *Biotemas*, vol. 26, no. 2, pp. 45–58, 2013.

[9] M. Quesada *et al.*, "Succession and management of tropical dry forests in the Americas: Review and new perspectives," *Forest Ecol. Manag.*, vol. 258, no. 6, pp. 1014–1024, 2009.

[10] J. Terborgh, *Diversity and the Tropical Rain Forest*. New York, NY, USA: Scientific American Library, 1992.

[11] M. Nageswara-Rao, J. R. Soneji, and P. Sudarshana, "Structure, diversity, threats and conservation of tropical forests," in *Tropical Forests*. Rijeka, Croatia: InTech, 2012, pp. 3–18.

[12] H. Puig, *La fôret tropical humide*. Paris, France: IRD, 2007.

[13] V. Trichon, "Hétérogenité spatiale des structures en forêt naturelle de basse altitude à Sumatra, Indonésie," *Thesis de doctorat*, Toulouse, France: Université Paul Sabatier, 2006.

[14] I. M. Turner, "Species loss in fragments of tropical rain forest: A review of an evidence," *J. Appl. Ecol.*, vol. 33, pp. 200–209, 1996.

[15] G. Williams-Linera, "Vegetation structure and environmental conditions of forests edges in Panama," *J. Ecol.*, vol. 78, pp. 356–373, 1990.

[16] V. Trichon, "Cartographie d'une canopée de forêt tropicale par photographies aériennes numériques et analogiques," in *Proc. Biologie d'une canopée d'une forêt équatoriale III. Pro-natura international & Op´weration Canopée*, 1998, pp. 26–36.

[17] B. Koch, "Status and future of laser scanning, synthetic aperture radar and hyperspectral remote sensing data for forest biomass assessment," *ISPRS J. Photogramm. Remote Sens.*, vol. 65, no. 6, pp. 581–590, 2010.

[18] E. Næsset, "Estimating timber volume of forest stands using airborne laser scanner data," *Remote Sens. Environ.*, vol. 61, no. 2, pp. 246–253, 1997.

[19] J. Hyyppä and M. Inkinen, "Detecting and estimating attributes for single trees using laser scanner," *Photogramm. J. Finl.*, vol. 16, no. 2, pp. 27–42, 1999.

[20] E. Næsset, "Predicting forest stand characteristics with airborne scanning laser using a practical two-stage procedure and field data," *Remote Sens. Environ.*, vol. 80, no. 1, pp. 88–99, 2002.

[21] M. Maltamo *et al.*, "Identifying and quantifying structural characteristics of heterogeneous boreal forests using laser scanner data," *Forest Ecol. Manag.*, vol. 216, nos. 1–3, pp. 41–50, 2005.

[22] W. Ni, G. Sun, K. J. Ranson, Y. Pang, Z. Zhang, and W. Yao, "Extraction of ground surface elevation from ZY-3 winter stereo imagery over deciduous forested areas," *Remote Sens. Environ.*, vol. 159, pp. 194–202, 2015.

[23] R. Kadmon and R. Harari-Kremer, "Studying long-term vegetation dynamics using digital processing of historical aerial photographs," *Remote Sens. Environ.*, vol. 68, no. 2, pp. 164–176, 1999.

[24] E. Baltsavias, A. Gruen, H. Eisenbeiss, L. Zhang, and L. T. Waser, "High-quality image matching and automated generation of 3D tree models," *Int. J. Remote Sens.*, vol. 29, no. 5, pp. 1243–1259, 2008.

[25] R. N. Treuhaft and S. R. Cloude, "The structure of oriented vegetation from polarimetric interferometry," *IEEE Trans. Geosci. Remote Sens.*, vol. 37, no. 5, pp. 2620–2624, Sep. 1999.

[26] M. Pardini, A. Cantini, F. Kugler, K. Papathanassiou, and F. Lombardini, "Monitoring dynamics in time of forest vertical structure with multibaseline PolInSAR data," in *Proc. 2014 IEEE Geosci. Remote Sens. Symp.*, 2014, pp. 3366–3369.

[27] M. Neumann, L. Ferro-Famil, and A. Reigber, "Estimation of forest structure, ground, and canopy layer characteristics from multibaseline polarimetric interferometric SAR data," *IEEE Trans. Geosci. Remote Sens.*, vol. 48, no. 3, pp. 1086–1104, Mar. 2010.

[28] D. H. T. Minh *et al.*, "SAR tomography for the retrieval of forest biomass and height: cross-validation at two tropical forest sites in French Guiana," *Remote Sens. Environ.*, vol. 175, pp. 138–147, 2016.

[29] X. Yu *et al.*, "Comparison of laser and stereo optical, SAR and InSAR point clouds from air- and space-borne sources in the retrieval of forest inventory attributes," *Remote Sens.*, vol. 7, no. 12, p. 15809, 2015.

[30] D. Moe and R. Longhenry, "Metrically preserving the USGS aerial film archive," *Photogramm. Eng. Remote Sens.*, vol. 79, no. 3, pp. 225–228, 2013.

[31] I. S. Korpela and T. E. Tokola, "Potential of aerial image-based monoscopic and multiview single-tree forest inventory: a simulation approach," *Forest Sci.*, vol. 52, no. 2, pp. 136–147, Apr. 2006.

[32] H. Hirschmüller, "Stereo processing by semiglobal matching and mutual information," *IEEE Trans. Pattern Anal. Mach. Intell.*, vol. 30, no. 2, pp. 328–341, Feb. 2008.

[33] S. Narumalani, D. R. Mishra, and R. G. Rothwell, "Change detection and landscape metrics for inferring anthropogenic processes in the greater EFMO area," *Remote Sens. Environ.*, vol. 91, nos. 3–4, pp. 478–489, 2004.

[34] W. S. Hanson and I. A. Oltean, *Archaeology from Historical Aerial and Satellite Archives*. New York, NY, USA: Springer, 2013.

[35] M. T. Jorgenson, C. H. Racine, J. C. Walters, and T. Osterkamp, "Permafrost degradation and ecological changes associated with a warming climate in central Alaska," *Clim. Change*, vol. 48, pp. 551–579, 2001.

[36] C. Véga and B. St-Onge, "Height growth reconstruction of a boreal forest canopy over a period of 58 years using a combination of photogrammetric and lidar models," *Remote Sens. Environ.*, vol. 112, no. 4, pp. 1784–1794, 2008.

[37] K. Nurminen *et al.*, "Automation aspects for the georeferencing of photogrammetric aerial image archives in forested scenes," *Remote Sens.*, vol. 7, no. 2, p. 1565, 2015.

[38] USGS, "Landsat missions," *USGS Sci. Changing World*, 2013. [Online]. Available: http://landsat.usgs.gov/about_landsat1.php. Accessed on: Jan. 29, 2016.

[39] E. Dalponte Michele *et al.*, "Tree crown delineation and tree species classification in boreal forests using hyperspectral and ALS data," *Remote Sens. Environ.*, vol. 140, pp. 306–317, 2014.

[40] I. Korpela, "Geometrically accurate time series of archived aerial images and airborne lidar data in a forest environment," *Silva Fennica*, pp. 109–126, 2006.

[41] F. Remondino, M. G. Spera, E. Nocerino, F. Menna, and F. Nex, "State of the arte in high density image matching," *Photogramm. Rec.*, vol. 29, no. 146, pp. 144–166, 2014.

[42] P. R. Wolf and B. A. Dewitt, *Elements of Photogrammetry*, 3rd ed., Boston, MA, USA: McGraw-Hill, 2000.

[43] G. Durigan, "Métodos para análise de vegetação arbórea," in *Métodos de Estudos em Biologia da Conservação e Manejo da Vida Silvestre*, L. Cullen Junior, R. Rudran, and C. Valladares-Pádua, Eds., Curitiba, Brazil: UFPR; Fundação Boticário de Proteção à Natureza, 2003.

[44] I. C. G. Vieira *et al.*, "Classifying successional forests using Landsat spectral properties and ecological characteristics in eastern Amazônia," *Remote Sens. Environ.*, vol. 87, no. 4, pp. 470–481, 2003.

[45] P. Liao, T. Chen, and P. Chung, "A fast algorithm for multilevel thresholding," *J. Inf. Sci. Eng.*, vol. 17, pp. 713–727, 2001.

[46] J. L. Albuquerque Filho and C. B. B. Leite, "Elevações induzidas no lençol freático devido a formação de reservatórios e o significado das modificações resultantes," Geociências, vol. VII, no. 6, pp. 67–74, 2002.

[47] M. Chang, *Forest Hydrology: An Introduction to Water and Forests*. Boca Raton, FL, USA: CRC Press, 2003.

[48] M. G. Turner, "Landscape ecology: The effect of pattern on process," *Annu. Rev. Ecol. Syst.*, vol. 20, no. 1, pp. 171–197, 1989.

Adilson Berveglieri received the B.S. degree in mathematics from the State University of Londrina, Londrina, Brazil, and the B.S. degree in computer science from the São Paulo State University, Presidente Prudente, Brazil. He also received the M.Sc. and Ph.D. degrees in cartographic sciences from the São Paulo State University, Presidente Prudente, Brazil, in 2011 and 2014, respectively.

He is currently a Postdoctoral Researcher Fellow at São Paulo State University. His works are related to photogrammetry and image analysis.

Antonio Maria Garcia Tommaselli received the graduate degree in cartographic engineering from the Universidade Estadual Paulista Julio de Mesquita Filho, Presidente Prudente, Brazil, in 1983, the Master's degree in geodetic sciences from the Federal University of Paraná, Curitiba, Brazil, in 1988, the Ph.D. degree in electrical engineering from the State University of Campinas, Campinas, Brazil, in 1993, Habilitation by Unesp, Presidente Prudente, Brazil, in 1998, and a Postdoctorate from the University College London, London, U.K.

He is currently a Professor at the Universidade Estadual Paulista Julio de Mesquita Filho, Collaborator of the International Society for Photogrammetry and Remote Sensing and fellow FP 1C of the National Scientific and Technological Development Council. He has experience in geosciences with an emphasis on photogrammetry, acting on the following topics: digital photogrammetry, feature extraction, mapping and calibration of digital cameras.

Nilton Nobuhiro Imai graduated in Agricultural Engineering from the State University of Campinas, Campinas, Brazil, in 1979, the Master's degree in remote sensing from the National Institute for Space Research in 1986, and the Doctorate degree in geography (human geography) from the University of São Paulo, Presidente Prudente, Brazil, in 1996.

He is currently an Assistant Professor in the Universidade Estadual Paulista Julio de Mesquita Filho, Presidente Prudente. He has experience in geosciences, remote sensing with emphasis, mainly in remote sensing and GIS in the analysis and development of models for inferring the physical environment variables.

Eduardo Augusto Werneck Ribeiro received the B.S. degree in geography and the M.Sc. degree from the São Paulo State University, Presidente Prudente, Brazil. He received the Ph.D. degree in geography from Federal Univeristy of Paraná, Curitiba, Brazil, in 2011.

He is currently the Director of Research, Graduate Studies and Innovation of the Federal Institute of Santa Catarina, Blumenau, Brazil. His research interests include biogeography, thematic cartography, environmental monitoring, and public health.

Raul Borges Guimarães received the B.S. degree in geography from the Pontifical Catholic University of São Paulo, Perdizes, Brazil, and the M.Sc. and Ph.D. degrees in human geography from the University of São Paulo.

He is currently a Full Professor in the Department of Geography, São Paulo State University, Presidente Prudente, Brazil. His research topics are health geography, thematic cartography, urban and regional geography, and public politics.

Eija Honkavaara received the D.Sc. degree in technology in photogrammetry from Helsinki University of Technology, Espoo, Finland, in 2008.

She is currently a Research Manager and a Research Group Leader in the Department of Remote Sensing and Photogrammetry, Finnish Geospatial Research Institute, Masala, Finland. Her research interests include photogrammetry, unmanned aerial vehicles, radiometric and geometric calibration, computer vision, and hyperspectral environmental monitoring applications.